Effect of Modeling Complexities on Extreme Wind Hazard Performance of Steel Lattice Transmission Towers

Yousef Mohammadi Darestani^a, Abdollah Shafieezadeh^{b*}, and Kyunghwa Cha^c

^a PhD Candidate, Department of Civil, Environmental, and Geodetic Engineering, The Ohio State University, Columbus, Ohio, USA; Email: mohammadidarestani.1@osu.edu

^b Associate professor, Department of Civil, Environmental, and Geodetic Engineering, The Ohio State University, Columbus, Ohio, USA; Email: shafieezadeh.1@osu.edu

^c Graduate Student, Department of Civil, Environmental, and Geodetic Engineering, The Ohio State University, Columbus, Ohio, USA; Email: cha.142@osu.edu

*Corresponding Author: Abdollah Shafieezadeh

PhD, Associate Professor

Lichtenstein Endowed Professor of Civil, Environmental and Geodetic Engineering Risk Assessment and Management of Structural and Infrastructure Systems (RAMSIS) Lab

http://ramsis.osu.edu The Ohio State University

Department of Civil, Environmental, and Geodetic Engineering

214B Bolz Hall | 2036 Neil Ave | Columbus, OH 43210

Phone: 614-688-1559 | Fax: 614-292-3780

E-mail: shafieezadeh.1@osu.edu

CEGE Webpage: http://ceg.osu.edu/people/shafieezadeh.1

Effect of Modeling Complexities on Extreme Wind Hazard Performance of Steel Lattice Transmission Towers

Reliable computational models of transmission towers are key to improved hurricane risk management of transmission systems. However, a comprehensive understanding of involved complexities and their effects on the extreme wind performance of towers is not available. Particularly, buckling effects have not been captured properly and the failure of joints and the post buckling behavior of towers have not been investigated. Moreover, contributions of these and other complexities to key tower responses in the presence of uncertainties are not known. This paper presents an approach to modeling lattice towers that captures buckling and post buckling, and joint slippage and failure and analyzes their effects, while considering uncertainties, through a set of probabilistic, nonlinear pushover analyses in OpenSEES. Results for a double circuit lattice tower indicate that buckling can lead to 30% reduction in the load bearing capacity of towers. Joint slippage reduces the load bearing capacity of the tower by 6%. It also considerably increases tower displacement. Connection failure can also occur in rare cases and it subsequently, changes tower's failure mode. The proposed modeling approach can be used in risk analysis of transmission systems to investigate various performance levels and improve the design of towers.

Keywords: Power transmission system; steel lattice towers; Finite Element method; joint slippage; joint failure; pushover analysis

1. Introduction

Overhead electric transmission lines face substantial risk of damage in hurricane prone regions around the world. Past failures of these systems resulted in considerable economic losses as well as societal and organizational disruptions (Campbell, 2012; Hoffman and

Bryan, 2013). These events highlight the critical role of transmission systems in supporting power delivery to large geographical areas. High intensity wind-related hazard events such as hurricanes can result in different failure modes in transmission towers as these structures are composed of a large number of elements and connections with different behaviors. Moreover, uncertainties in the demand and capacity of transmission towers and the complex behaviors of tower elements including post yielding and post buckling behavior of the members, joint slippage, and joint failure, along with imperfections enlarge the space of potential failure modes (De Souza, 2019, Kempner et al., 2002). However, these complexities are commonly neglected in the design and analysis of transmission towers. For example, Tapia-Hernández et al. (2017) and Tapia-Hernández and Sordo (2017) investigated the collapse mechanism of transmission towers through pushover analysis. They observed that the failure is commonly associated with a stress concentration in the main vertical elements of the tower at the bottom or mid height of the tower. The stress concentration results in buckling of the elements, which subsequently leads to the collapse of the tower due to the development of a failure mechanism. Although the aforementioned studies tried to capture the nonlinear behavior of lattice towers, the effect of imperfection on the buckling capacity of steel elements as well as the effect of joint slippage and uncertainty (in material and loading) on the development of failure modes are not considered. Moreover, Jiang et al. (2011), performed pushover analyses of transmission towers by considering joint slippage and buckling effects. However, the model does not account for the effect of uncertainties in demand and capacity on the performance of towers. Imperfections, post yielding elasticity, and connection failure effects were not considered as well. Neglecting imperfections in the alignment of elements can induce errors in the estimation of buckling in steel elements, as the additional P-δ effects are not captured. Moreover, the generated

model appears to follow an elasto-plastic behavior and therefore does not account for post yielding elasticity. More recently, Jiang et al. (2017) investigated effects of joint slippage by enhancing their Finite Element model to consider imperfection effects. However, post yielding and post buckling effects, failure of joints, and effects of uncertainties were not captured in the model. In another recent study, Fu and Li (2018) performed a probabilistic analysis of transmission towers to develop wind fragility functions. These fragility models offer an important initial step toward reliability and risk analysis of transmission systems. However, the generated numerical model of towers does not consider joint slippage, joint failure, post buckling, and post yielding behaviors. The individual and collective effects of these factors can impact the emergence and likelihood of failure modes in transmission towers as load distribution and element stresses may not be estimated properly. Furthermore, the study assumes that if the displacement of the tower exceeds a predefined buckling displacement, the tower fails. The buckling displacement, there, is defined as the displacement corresponding to a significant change in the slope of pushover curve for a deterministic analysis of tower based on mean values of uncertain variables. However, according to the provided probabilistic pushover curves, for a large percentage of realizations, the tower can resist against further loading after the predefined buckling displacement is reached. This inconsistency in the definition and observations of failures in simulation results is, in part, due to the inability of the implemented Finite Element models to capture element and joint failures, and the propagation of nonlinearities because of load redistributions. This further highlights the need for reliable computational models for fragility and risk analysis purposes. Furthermore, Kaminski et al. (2008) investigated the impact of uncertainty (in material and loading) on member forces and top displacement of a transmission tower subjected to conductor failure.

However, the impact of uncertainty on the emergence and likelihood of failure modes is not investigated in that study.

A number of studies, in addition to sharing some of the modeling limitations explained earlier, conservatively underestimated the load bearing capacity of transmission towers. These studies assumed that any yielding or buckling in tower elements results in the complete failure of the structure (Rezaei et al., 2017; Rezaei et al., 2016; Tessari et al., 2017; Kroetz et al., 2017). As towers are statically indeterminate, failure of a single bracing does not necessarily result in the collapse of the tower as long as there is no failure mechanism in the system. Usually a failure mechanism is accompanied by the buckling of the main elements in the tower including the vertical elements in the cage or the leg elements. A handful of studies performed pushover analyses to obtain the load bearing capacity of towers. However, they failed to capture post peak behavior of towers in pushover curves (Jiang et al., 2011; Fu and Li, 2018). Characterizing such behaviors is important in establishing limit state functions for severe states of damage such as partial or complete collapse. This is in part due to the inability of their numerical models to handle highly nonlinear phenomena such as post yielding, post buckling, and complex joint slippage behaviors. In terms of considering joint slippage, a few studies used experimentally validated joint slippage models such as those developed by Ungkurapinan (2000). As pointed out in (Wang et al., 2017), these models however do not accurately represent the actual joints used in transmission towers, as the number, type, and capacity of bolts as well as the dimension of elements and steel material properties are different from one joint to another. Therefore, the few models presented by Ungkurapinan (2000) cannot cover all these variations. In order to overcome this issue, Wang et al. (2017) leveraged the capabilities of ANSYS Finite Element software to model joints embedded in their Finite Element model. Although this method results in an

accurate estimation of joint slippage behavior, the computational cost associated with adding contact elements that can capture joint slippage behavior is considerably expensive. In order to avoid this issue, Wang et al. (2017) limited their joint models to only a few connections in the tower and neglected the joint slippage behavior for the rest of the connections. This issue exacerbates in the case of probabilistic analysis of transmission towers where a large number of simulations are required.

In order to address the aforementioned limitations, the current study investigates the effect of different complexities on the load bearing capacity and emergence of failure modes. For this purpose, six different models with varying levels of complexity are generated. Among these models, the simplest neglects buckling and joint slippage and the most complex one considers buckling, joint slippage and joint failure. Detailed information about these models are provided in the numerical study section. Moreover, the impact of various uncertainties on the performance of towers is investigated by performing a set of nonlinear static pushover analyses in OpenSEES (McKenna, 2000) Finite Element platform through 200 realizations of uncertain variables generated by Latin Hypercube Sampling (LHS) method for each of the six models. The considered complexities include post buckling and post yielding behavior of tower elements, nonlinear joint slippage models with different clearance levels, and the failure of joint. Uncertainties include those associated with steel material behavior, imperfections, joint slippage behavior, and wind induced loadings. In order to account for out-of-plane displacements of steel elements and associated P-8 effects, large deformations are accounted for via a co-rotational geometric transformations. To take full advantage of large deformations to accurately capture buckling effects, each element is divided into four sub-elements modeled with displacement-based beam column elements. This element discretization accurately captures the out of plane displacements when the

element buckles. Additionally, an initial camber displacement is applied to the mid-nodes of each element to account for imperfection effects. In this study, based on the joint slippage model of Ungkurapinan (2000), a modeling approach for joints is proposed that can accurately account for the impact of joint slippage as well as joint failure in lattice towers. For this purpose, three hysteretic material models in OpenSEES are put together in parallel to generate the nonlinear force-deformation behavior of connection reported in Ungkurapinan (2000). This model is then extended to account for joint failure by reducing the load capacity of the connection after reaching the maximum capacity. It should be noted that the joint slippage models suggested by Ungkurapinan (2000) are not necessarily representative of the accurate joint slippage behaviour in the assumed lattice tower. However, in terms of general backbone behavior, bolt numbers, and configuration, they match the joints in the lattice tower assumed in this study.

A 27.4 m double circuit vertical steel lattice tower is considered to perform the analyses. This type of steel tower is one of the most common towers in the US. For each realization of uncertain variables, a nonlinear static pushover analysis is performed and therefore, 200 pushover curves are obtained. The pushover analysis can provide better insights regarding the impact of uncertainties and various modeling complexities on the load bearing capacity, failure modes, and force-displacement behavior of transmission towers. As the proposed modeling approach is able to handle highly nonlinear post peak load behaviors, it can be easily used to investigate different performance levels of lattice towers. This will help in risk and life cycle cost analysis of transmission lines as the incurred cost is a direct function of the type and extent of damage to lattice towers.

2. Finite Element (FE) Modeling of Lattice Transmission Towers

Overhead lattice transmission towers exhibit complex behaviors under wind loadings. This complexity in part stems from the fact that a large number of components in lattice towers experience material and geometric nonlinearities especially under strong wind loadings such as hurricanes. Although during high intensity wind hazard scenarios, a tower may experience various levels of damage, as long as conductors are supported with a safe distance from each other and earthed objects, the transmission of electricity will not be interrupted. Therefore, from power delivery perspective, it is important to distinguish damage from collapse. A collapse in a transmission tower often occurs when a failure occurs in the main elements of the tower. This could be due to buckling or yielding of a couple of elements in the leg such that the tower overturns, or it could be due to the failure of vertical elements in the cage or failure of the cross arms such that the conductors are no longer supported leading to the disruption of power delivery. In order to capture these complex behaviors and reliably identify and characterize the various modes of failure, high-fidelity Finite Element models for lattice transmission towers are required. Toward this goal, a modeling procedure is proposed here that is capable of considering material nonlinearity, P- δ and P- Δ effects, buckling due to imperfections, and nonlinear joint slippage behavior and the failure of bolted connections. In the following subsections, different modeling aspects of the proposed nonlinear Finite Element modeling of transmission towers are presented.

2.1. Steel Elements

Steel lattice towers are mainly constructed by steel angle members and bar elements.

Although under service loads steel elements act approximately as linear elastic elements, under severe loads such as strong winds, steel elements can undergo buckling and post

yielding behavior. Since the objective of this paper is to identify different failure modes in transmission towers, it is imperative to accurately capture the post yielding behavior of steel elements. OpenSEES Finite Element platform is capable of modeling nonlinear steel elements by a broad library of materials that can account for nonlinear behavior. Among these models, "steel01" material model considers a bilinear material model. The behavior of this model is defined with modulus of elasticity, E, yield stress, f_y , and post yield elasticity, E_{st} . In order to define tower elements, displacement-based nonlinear beam-column elements and force-based nonlinear beam-column elements can be considered. Both elements consider plasticity at multiple points along the length of the element through defining integration points. In addition, at each integration point, the section of the element is divided into multiple fiber elements along the height and width of the element. Each fiber acts as an individual element with a unique material behavior and cross sectional area. Therefore, at each cross sectional area different fiber elements can undergo different level of loading. Subsequently, bending moments and axial stresses can be accurately distributed along the fibers to represent the actual force distribution at each integration point. In this case, plastic deformations can be accurately estimated. Since displacement formulation provides better convergence during nonlinear analyses, in this study, displacement-based beam-column elements are utilized. For each element, 5 integration points are defined and the fiber sections associated with each integration point uses "steel01" material with 10 fibers along the height of angles and 3 fibers along the width of angles. The number of fibers is in line with the experimentally validate models suggested by Uriz et al. (2008).

2.2. Buckling

Buckling in lattice elements can considerably contribute to the overall performance of towers. A number of previous investigations identified buckled elements in numerical models based on design code recommendations for maximum compressive forces (Rezaei et al., 2016; Tessari et al., 2017; Kroetz et al., 2017). However, this approach has limited application as the formulas suggested in design codes are approximate. In addition, the analyzed performance of the tower is only valid until the first buckling occurs and the produced Finite Element (FE) model will not be able to accurately capture the behavior of the tower post the first element buckling. In another study, Jiang et al. (2011) used the capabilities of USFOS (2003) Finite Element platform to model buckling effects. For this purpose, each element is modeled using a single nonlinear beam element and the stresses are checked at the ends and mid length of the element. If the stress at each of these points exceeds the yielding stress, a plastic hinge is assigned to the corresponding point. Although this approach provides a better estimation of buckling effects, it is not able to account for imperfections and post buckling effects. The imperfection effects are not accounted for as the elements are modeled using a single **straight** element. Post yielding effects are not considered as well because the plastic hinges appear to follow an elastoplastic behavior without any post yielding elasticity. In addition, in order to accurately estimate buckling effects, large deformations should be considered in the Finite Element analysis. However, large deformation effects appear to be neglected in the analysis. In another study, Jiang et al. (2017) used NIDA (2011) Finite Element platform to account for buckling effects. NIDA is capable of considering P- δ and P- Δ effects. P- δ effects account for additional loading caused by initial bowing and P-Δ effects account for additional loading caused by frames lateral displacement (Jiang et al., 2017). Similar to USFOS, it seems that this model cannot account for large deformations. In addition, the

post yielding behavior of elements cannot be captured as the model is not capable of considering post yielding elasticity of tower elements. Therefore, this model is not able to accurately estimate the buckling effects.

In order to capture buckling appropriately, imperfections, P- Δ and P- δ effects, and large deformations should be considered. OpenSEES Finite Element platform is capable of considering buckling in the system. According to Uriz et al. (2008) to account for buckling in OpenSEES, each element should be divided into at least two inelastic beam-column elements with at least three integration points. In addition, 10-15 layers of fibers along the height and 3-5 layers of fibers along the width of each section should be considered. Moreover, the middle node should have an initial camber displacement of 0.05~0.1% of the original length of the element. The middle node is essential in the large displacement formulation in order to account for in-plane and out-of-plane deformations in the middle of the element (Uriz et al., 2008). In addition, in order to account for geometric nonlinearities, large deformations should be considered through a "Corotational" geometric transformation in OpenSEES. Uriz et al. (2008) validated their inelastic buckling model by a set of cyclic loading experiments performed by Black et al. (1980).

The model suggested by Uriz et al. (2008) in terms of the number of element discretizations was examined for the tower elements used in this study. It was observed that although breaking each element into half provides better estimates for the buckling force in tower elements, to obtain an acceptable accuracy for the buckling behavior of angle section elements, more discretizations are required. For this purpose, a single element with two different boundary conditions was modelled in OpenSEES as shown in Fig 1. In the first model, it is assumed that both ends of the element are pinned (Fig. 1.a) and in the second model it is assumed that both ends are fixed. These two models are

representative of two extreme cases. In transmission towers, the elements are connected to one another using bolts. Depending on the number of bolts, capacity of the bolts, and the pre-tensioning force in the bolts, the boundary conditions for each element follows a semi-rigid connection somewhere between the two extreme cases presented in Fig. 1. If the buckling model works for both extreme cases, it is expected that it will capture the behavior for all the elements in the transmission tower. Table 1 and Table 2 provide the result of a convergence study on the effect of number of discretizations and imperfection camber displacement on the buckling force of a 1.75X1.25X0.1875 angle section for the simply supported and fixed end models, respectively. This element is one of the smallest sections in the tower. It is 3.024 m long with a yield stress of 245.6 MPa and a modulus of elasticity of 192.1 GPa. The results show that for the simply supported beam, four elements yields 2.4% error using 0.001L camber displacement in the middle. For the fixed end beam, four and eight elements yield 15.5% and 1% error, respectively. The results of the convergence study for a 4X4X0.3125 angle section beam are also presented in Tables 3 and 4. This section is one of the strongest sections used in the transmission tower. The length of the element is 1.55 m and the material properties of the section is the same as those for the 1.75X1.25X0.1875 section. For a simply supported beam, four elements yield 0.2% error, while for the fixed end beam, two elements result in 5.9% error. Therefore, for the range of the elements used in the current study, if each tower element is discretized into eight sub-elements, the accuracy of the model in terms of capturing the true buckling force is guaranteed. However, it should be noted that discretizing the elements into eight sub-elements will considerably increase the computational demand. This becomes especially challenging in case of reliability analysis as they require a large number of simulations. On the other hand, four sub-elements can provide a faster analysis without considerable loss of accuracy, as four elements yield

moderate error only for the case of the fixed end beam for 1.75X1.25X0.1875 angle section. However, the rigidity of the connections for smaller sections that are usually used as bracing elements with one bolt is closer to a pinned connection. Therefore, the maximum error is closer to 2.4%. Subsequently, in this study, for the analysis of the tower, each element is divided into four sub-elements to provide a sufficiently accurate model with reduced computational costs. A sketch of the discretization model of each element is provided in Fig. 2. It should be noted that to account for the effect of uncertainty, the imperfection value in the mid-node is assumed to follow a uniform distribution between 0.05% and 0.1% of the length of the element. In addition, the shape function for Euler buckling force is defined as $\varphi = sin(\pi x/L)$, where x is the distance from the left side end of the element. The value of the imperfection at each node is calculated accordingly. For the current analysis that discretizes each element into four sub-elements, the value of imperfection at the first, and third node is obtained as 0.707 of the imperfection in the mid-node (Fig.2)."Moreover, the buckling force is a function of the inverse of KL/r, where K is the column effective length factor, L is the unsupported length, and r is the radius of gyration. For an element with the same unsupported length along all axes (same K along all axes), the smallest radius of gyration results in the lowest stress that causes buckling in the element. The radius of gyration for the weakest axis is the smallest, therefore, elements tend to buckle along their weakest axis. To capture this behavior, the imperfection was applied perpendicular to the weakest axis of L-section and bar elements (as shown in Fig. 3) as the imperfection applied perpendicular to the weak axis causes additional moment along the weak axis.

Eccentricity also impacts the buckling capacity of tower elements as it induces additional moment in the elements. There are two eccentricities in transmission towers. The first form of eccentricity is where elements are connected to one another such that the lines passing through the centers of gravity of the sections do not coincide. However, according to Fang et al., (1999), transmission towers are designed such that such eccentricities are avoided. This is achieved by aligning bolted connections using gusset plates. The second form of eccentricity exists in joints with bolts in one leg of angle elements. As OpenSEES automatically aligns elements along their centroid, there is no straightforward approach to account for such eccentricities in OpenSEES. In order to accurately account for eccentricities, additional nodes should to be defined in the vicinity of each joint. The new nodes should be located at a distance equal to the eccentricity of the elements and subsequently it should be connected to the joint using rigid link elements. This process becomes significantly challenging especially for transmission towers where there are a large number of connections. In addition, defining additional nodes increases the complexity and the computational costs of the Finite Element analysis as the dimension of the stiffness matrix drastically increases by adding additional nodes. Therefore, in this study the effect of eccentricity due to bolts in one leg of the angle section is neglected.

2.3. Joint Slippage and Joint Failure Model

In performance assessment of transmission towers, joints are commonly simplified as rigid or pinned connections (Rezaei et al., 2016; Tessari et al., 2017; Kroetz et al., 2017). However, under strong wind loadings such as hurricanes, joints slippage occurs, which is a nonlinear phenomenon. A few studies provided slippage behavior of bolted joints by performing a set of static load tests (Kitipornchai et al., 1997; Ungkurapinan, 2000). The

experimentally validated model developed by Ungkurapinan (2000) have been used in the previous studies on the impact of joint slippage of bolted connections in steel lattice towers (Jiang et al., 2017; Jiang et al., 2011). The study also provides uncertainties of key points in the force-deformation behavior of the connections as well as different clearance levels for the arrangement of the bolts. Although connections can fail under service and severe loadings, in all the previous studies, joint failure mode is neglected. The three connection models proposed by Ungkurapinan (2000) are shown in Fig. 4. Connection Type A models a compression joint in transmission line towers. Therefore, it can accurately approximate the slippage behavior of lap splices in the main legs of the tower. The backbone curve for connection Type A is provided in Fig. 5.a. This backbone behavior consists of four phases. In phase 1, the connection acts as an elastic element due to a static friction between the angle elements. If the axial force becomes as large as the friction force between the two angles, the angles start to slip with reduced frictional stiffness (phase 2). Subsequently, if the slippage is large enough that the bolts make contact with the edges of the holes, due to the load bearing of the bolts, a higher stiffness is observed (phase 3). Moreover, if the load becomes large enough, a plastic deformation can occur in the angle elements or bolts and a nonlinear behavior is observed in the backbone curve of the connection until the connection fails (phase 5). Connection Type B model was designed for representing tension joints. A schematic backbone curve of this model is presented in Fig. 5.b. Ungkurapinan (2000) observed that unlike connection Type A, in the second phase of the backbone curve of connection Type B, stiffness is very small and a nearly pure slippage occurs in the model. Therefore, the forces at the initial and end points of this phase are identical (Phase 2 in Fig. 5.b). Connection Type C represents simple joints in transmission towers where there is no gusset plates or splice angles. The backbone curve of this model is similar to connection Type B, which has a pure slippage in phase 2 (Fig. 5.b). Another important consideration in the slippage behavior of connections is the level of clearance for joint bolts. Due to construction limitations, commonly, holes are made slightly larger than the diameter of bolts. This increase in the diameter of holes helps construction workers to fit bolts into the holes much easier. Ungkurapinan (2000) also investigated the impact of construction clearance on the slippage behavior of bolted connections. It was observed that the construction clearance affects the deformation length for phase 2 of slippage. The construction clearance was categorized into three levels called minimum, normal, and maximum clearance (Fig. 6).

As noted earlier, the current study adopts the model developed by Ungkurapinan (2000). Therefore, three connection types in the tower are considered. The first connection is the lap splices for the legs of the tower. For this connection, Type A connection model proposed by Ungkurapinan, (2000) is considered (Fig.7.a). Second connection is the connection of bracing elements to each other (Fig. 7.b). In order to model this connection, connection Type B suggested by Ungkurapinan (2000) is chosen. Finally, the third connection is the connection of bracing elements to the main elements (Fig. 7.c-e). In this study, connections of bracing to main elements are made with one, two, and three bolts. Since Ungkurapinan (2000) provided models for connection Type C with one to four bolts, for the connection of bracing elements to the main elements, connection Type C is considered.

To model joint slippage behavior of joints, Zerolength elements are used in OpenSEES. Zerolength elements can be defined between two nodes with identical coordinates. The direction of each Zerolength element can be specified by defining its local axes. Therefore, in order to define a joint slippage model, two nodes should be defined at the location of the connection. Subsequently, a Zerolength element can be

applied between the two nodes (Fig. 8). It should be noted that the nodes defined for the Zerolength elements and shown in Fig. 8 are actually located at the same point. In Fig. 8 only for showcasing the direction of connections the nodes are shown in non-identical locations. Moreover, local axis of the Zerolength element should be defined such that the local x direction is parallel to the direction of slippage. For each Zerolength element, three transitional and three rotational local axes can be defined. The slippage model should be applied along local x axis of Zerolength element and a large stiffness is applied to other transitional local axes to prevent any relative displacement in other transitional degrees of freedom.

In order to have a reliable assessment of the slippage behavior of connections, it is imperative to have a force-deformation model that can accurately estimate the nonlinear connection models presented in Fig. 5. OpenSEES platform is not able to directly model this complex behavior. However, OpenSEES provides the capability of combining different materials in parallel and series formations. In addition, since in nonlinear pushover analyses, there might be multiple unloading in the elements that are already yielded or buckled, the material model should be capable of modelling hysteretic behavior in the connections. In order to generate the required joint slippage model, three hysteretic materials are defined in parallel configurations as shown in Fig. 9. As seen in Fig. 9, the assumed model is able to accurately approximate the model proposed by Ungkurapinan (2000). Moreover, the proposed model is capable of capturing failure in the connections by reducing the capacity of the connection to α times the max load capacity of the connection as it is shown is Fig. 9. While the configurations of the joints in the considered tower are close to those studied experimentally by Ungkurapinan (2000), they may not be exactly the same for all connections. However, for the purposes of this study, the implemented models can estimate the general impact of joint slippage with an acceptable accuracy. The only adjustment applied to the connection model compared to the model suggested by Ungkurapinan (2000), is in the lap splices (connection Type A), where there are a total of eight bolts in the connection. However, the closest model presented by Ungkurapinan (2000), has a maximum of four bolts. For this particular connection, since the angle elements are the same, the capacity of the connection is adjusted. For this purpose, the force capacity of the joint at point D in Fig. 5.a. is found as the minimum of the capacity of eight bolts, capacity of the gross angle section using the yield stress of the element, and the ultimate capacity of the net (punched) angle section using the ultimate stress of the element. The force capacity of points B and C are adjusted proportionally from the model suggested by Ungkurapinan (2000). In addition, the force capacity of point A in Fig. 5.a. is found by doubling the value suggested by Ungkurapinan (2000) as this value is only affected by the number of bolts. For this connection, the same displacement values suggested by Ungkurapinan (2000) are used as the displacement of each phase is not affected by the number of the bolts.

It should be noted that in practice, joints are designed such that their capacity is higher than the capacity of the connected elements and therefore, it is expected that the connections do not fail as elements should fail first. However, considering uncertainties in connection capacity and construction errors, among other factors, there is a small probability that a failure can occur in the joints. Therefore, as this study analyzes the extreme performance of transmission towers with a probabilistic perspective, the chance of failure in the connections cannot be neglected. For this purpose, the Finite Element model should also be able to account for failure in connections.

2.4. End Moment Conditions at Joints

The rigidity of connections in terms of transferring moments is a function of the number

of bolts, the arrangement of the bolts, the pre-tensioning force, and the capacity of the bolts. In design and analysis of transmission towers, it is commonly assumed that joints are either pinned or fixed in rotational degrees of freedom. Although the assumption of pinned connection is valid for joints with one bolt, it is not the case for connections made of more than one bolt. For these joints, the moment-rotation behavior of the connection can be obtained as a function of the force-deformation behavior of the same connection with one bolt. Let's consider a bolt connection as presented in Fig. 10.a, for each bolt in the connection, here, it is assumed that the force-deformation behavior follows a backbone curve as previously shown in Fig. 5. An assumption here is that bolt holes have circular shape, therefore, independent of the direction of the slippage, the same backbone force-deformation applies for the bolt. In addition, it is assumed that the failure of joints is due to the plastic deformation in bolts and not angle sections. Considering the force-deformation in Fig. 5, the contribution of one bolt in the connection to its moment resistance can be derived as:

$$M = F.r \tag{1}$$

where F is the force capacity of the joint presented in Fig. 5 and r is the distance between the center of the bolt and the center of the connection (Fig. 10.a). In addition, the rotation (θ) of each bolt is a function of the displacement (δ) of the bolt presented in Fig. 5 as:

$$\theta = \delta/r \tag{2}$$

The resulting moment-rotation curve for the contribution of a joint to the connection behavior is shown in Fig. 10.b. Because bolts in connections work in parallel, the derived moment-rotation relations for individual bolts are combined in parallel to define the moment-rotation relationship of the joints. It should be noted that the moment capacity of single bolted connections is zero, therefore, they are modelled as pin. In addition, for lap splices as both sides of the angle sections are connected with four bolts on each side,

the behavior is very close to a fixed connection. Therefore, a fixed connection in rotational degrees of freedom is assumed for lap splices.

3. Wind Load on Lattice Towers and Conductors

Wind load on transmission towers depends on a number of factors, including velocity and direction of the wind, configuration, and geometry of towers. To determine wind loads on transmission towers, the static equivalent gust wind load model in ASCE07 (2016) is adopted here. According to this model, the wind force per unit length for a non-building structure can be determined using:

$$f_w = q_z G C_f D (3)$$

where q_z is the velocity pressure at height z on the tower, G is the gust-effect factor, C_f is the force coefficient, and D is the diameter perpendicular to the wind direction. The wind velocity pressure is calculated from:

$$q_z = 0.613K_z K_d K_{zt} K_e V^2 (4)$$

where K_z is the velocity pressure exposure coefficient, K_d is the wind directionality factor, K_{zt} is the wind topographic factor, K_e is the elevation factor, and V is the 3-second gust wind velocity at 10 m above the ground line. K_z is a function of the height from the ground line and exposure category and is calculated from

$$K_z = 2.01 \left(\frac{\max(4.75, z)}{z_g}\right)^{2/\alpha}$$
 (5)

where z is the height from the ground line, assuming the transmission line is located in an open terrain area, the exposure category is C, and α and z_g are 9.5 and 274.32 m, respectively (ASCE07, 2016). Although Eq. (3) has been developed for atmospheric wind loads, it offers a reasonable load pattern for hurricane-induced loads and it is widely used as the hurricane load pattern ASCE07 (2016). K_d , K_e , and K_{zt} are taken as 1 (ASCE07,

2016). The gust-effect factor, G, accounts for the effects of the dynamic nature of wind forces on the tower. In the case of the transmission tower, G is set as 0.85. According to ASCE07 (2016) the force coefficient, C_f , for squared trussed towers is calculated as

$$C_f = 4 \in^2 -5.9 \in +4 \tag{6}$$

where \in is the ratio of solid area to gross area of the tower face under consideration. In addition, a force coefficient equal to 1 is considered for conductors (ASCE 74, 2009).

4. Uncertainties and Probabilistic Simulations

Most of the current studies consider deterministic models to investigate the performance of towers (Jiang et al., 2017; Jiang et al., 2011). Although deterministic models provide insights about the average behavior of towers, they cannot account for variations in the demand and capacity and therefore, they cannot identify different failure modes in a transmission tower. There are different uncertainties in modelling of transmission towers. Steel material properties, wind loads, cross sectional areas, joint slippage models, and imperfections, are uncertain variables. Although towers are commonly designed to fail under buckling of leg elements (Tapia-Hernández et al., 2017), uncertainty can affect the performance of towers by changing the level of demand and capacity on the elements of the structure, and therefore, the structure as a system. Consequently, if uncertainties are considered, it is expected that for a percentage of realizations of the structure and loads, other failure modes will emerge. Subsequently, it is imperative to investigate the performance of transmission towers considering all uncertainties involved in modelling of these structures.

In order to investigate the impact of uncertainties on the performance of towers, a probabilistic approach is required. A Monte Carlo simulation approach is adopted here to generate realizations of uncertain variables and investigate effects of uncertainties on the

emergence of failure modes. The behavior of steel is defined with the modulus of elasticity E, yield stress f_y , and post yield elasticity E_{st} . The distribution type, mean and coefficient of variation (COV) for these random variables are presented in Table 5. In addition, imperfections are considered to be uncertain. It is assumed that imperfections follow a uniform distribution between 0.0005-0.001 of the length of the element (Uriz et al. 2008). Furthermore, it is assumed that all elements in a tower have the same material properties; however, imperfection values are different. This is mostly due to the high variability in imperfection since construction and assembly of elements induce random imperfections. On the other hand, the elements used to construct the tower are usually made from the same stack of steel profiles where their properties are considerably close to one another. Although in a single realization, all elements are modeled with the same material properties, the material properties from one realization to another is modeled probabilistically using Latin Hypercube Sampling (LHS) method.

Uncertainties in the variables defining wind pressures on tower elements are also included. The probabilistic model proposed by Ellingwood and Tekie (1999) is adopted to obtain the probabilistic model of each uncertain parameter defining wind load pressures. Gust effect factor, force coefficient, velocity pressure exposure coefficient and wind directionality factor are the uncertain variables in Ellingwood and Tekie (1999) and are included in this study. Table 5 presents the probability distribution model and COV of the random variables adopted from Ellingwood and Tekie (1999). The mean value of these uncertain variables are obtained from section 3.

As mentioned earlier, Ungkurapinan (2000) performed a set of experiments and reported the mean and standard deviation of variables defining the nonlinear slip behavior of connections. This study adopts these probabilistic models to investigate impacts of uncertainties in the connections behavior on the performance of lattice towers.

Ungkurapinan (2000) only reported the mean and standard deviation of key variables on force-deformation curves. However, the probability distribution model is not reported. Since the uncertain variables are all nonzero, a lognormal distribution is assumed to define the probability distribution models. Therefore, all variables except the slippage length are defined by a lognormal distribution. For the slippage length, Ungkurapinan (2000) considered three levels of clearance and based on each clearance level, a slippage length was obtained. However, the clearance level can be any value between the minimum and maximum clearance limits. Therefore, instead of defining three clearance levels, in this study, a uniform distribution is considered for the slippage length. The minimum and maximum values of the slippage length correspond to the minimum and maximum clearance levels, respectively. The distribution, mean and COV of each uncertain parameter defining the slippage behavior of connections Type A-C are provided in Table 6.

5. Numerical Study

5.1 Configuration of the tower

In performance assessment of transmission towers, uncertainties in material properties, connection behavior, and wind-induced loadings may affect the emergence of different failure modes. Deterministic analysis methods are not capable of identifying many of failure modes. In order to address this limitation, probabilistic analysis procedures such as Monte Carlo simulation method are required to account for various uncertainties in demand and capacity of the system. In this section, a Monte Carlo simulation approach is adopted to investigate the influence of uncertainty on the performance of the system and associated failure modes in transmission towers. For this purpose, an actual 27.4 m double circuit steel lattice tower located in a hurricane prone coastal area in south of the United

States is considered for nonlinear static pushover analysis. Double circuit steel lattice towers are commonly used in coastal regions of the United States. Therefore, the chosen tower is representative of a large percentage of lattice towers in hurricane prone regions. Investigating the performance of this tower can provide a better understanding regarding the performance of transmission towers in hurricane prone regions. A sketch of the modelled tower is provided in Fig. 11. It is assumed that two lines of three phase conductors at three cross arm levels and two lines of neutrals at the top are carried by the tower. Therefore, a total number of eight conductors are carried by the line. The three phase conductors have an overall diameter of 28.1 mm with a 1627 kg/km weight. These conductors are called Drake based on US naming system for Aluminum Conductor Steel reinforced (ACSR). In addition, the neutrals are optical ground wires (OPGW) with a diameter of 13.4 mm. The span length of conductors is 258 m. It is assumed that multiple spans with identical towers, conductors, and span lengths exist in the transmission line system. If the properties of adjacent spans in a line are identical, the structural couplings between the adjacent spans are not significant and can be neglected (Darestani et al., 2016a; Darestani et al. 2016b; Darestani et al. 2017; Darestani and Shafieezadeh, 2017; Bhat et al., 2018; Darestani and Shafieezadeh, 2019a; Darestani and Shafieezadeh, 2019b). Subsequently, in this study, a single transmission tower is modeled without any conductors attached to it. However, the gravity and wind induced loadings from conductors attached to the tower are applied at the intersection of cross arms and insulators as point loads. The gravity and wind induced loadings are distributed equally between adjacent towers. Therefore, to calculate point loads of conductors on the tower, an effective span length of 258/2=129 m is considered for conductors at each side of the tower. Subsequently, an overall effective span length of 258 m is considered for gravity and wind load calculation for each line of conductor on the tower. It is also assumed that there is no horizontal angle in the horizontal plane between the conductors at each side of insulators. Therefore, there is no unbalanced loading at the insulator location due to the tensile force in the conductors. In addition, the failure of conductors is not considered in this study, therefore, the associated unbalanced conductor load is not considered. This unbalanced load will be addressed in future investigations. The tower is initially designed to withstand a wind speed of 130 mph. This wind speed is used as the reference load factor in the pushover analysis. Therefore the load factor of 1 corresponds to the 130 mph design wind speed. In this section, a probabilistic pushover analysis investigates the performance of the tower through 200 realizations of uncertain variables generated by Latin Hypercube sampling (LHS) method with uncertain material, connection, imperfection, and wind load models defined in sections 2-4. Subsequently, each tower is analyzed in OpenSEES Finite Element platform.

5.2 Effect of modelling complexities on force deformation behavior of the tower

In order to investigate the effect of modelling complexities, six different models presented in Table 7 are developed in OpenSEES. In model NBUCL&NSLIP rigid connections are considered and the buckling effect is not captured. Model BUCL adds buckling effect to model NBUCL&NSLIP. Model SLIP does not consider buckling, but it considers joint slippage effect. In this model, connections are modeled by setting α in Fig. 9 as 1. In this case, there is no drop in the backbone curve of the connection and therefore, this model is not capable of capturing failure in connections. However, model SLIPF sets α as 0.25. Therefore, model SLIPF is capable of capturing failure in connections. Model BUCL&SLIP considers both buckling and joint slippage. However, this model considers

 α as 1 and therefore, it is not capable of capturing failure in joints. Model BUCL&SLIPF, which is the most accurate model, considers buckling, joint slippage and, and joint failure. Similar to model SLIPF, this model considers α as 0.25. To consider the effect of wind direction on the performance of the tower, wind is applied to the tower in transverse and longitudinal directions. When a longitudinal direction is considered, wind induced loading on conductors is zero because the wind is parallel to conductors. When a transverse direction is considered, wind induced loading on conductors is maximum as the projected wind surface area on conductors is maximum. In this study, a displacementcontrol pushover analysis is performed using OpenSEES. For this purpose, the displacement of the top of the tower is initially increased with 1 mm increments and the equivalent load that causes the corresponding displacement is calculated using Newtown line search method. The tolerance limit for the Newton line search method is set as 1e-5. If the analysis does not converge using the initial displacement increment, the solver reduces the displacement increments in several steps. In this study, the displacement increment is reduced 5, 10, 100, 1000, and 10000 times until the convergence is achieved. If the convergence is not achieved, the solver tries Newton with initial tangent, and Broyden methods that are available in OpenSEES. Using the aforementioned solver on a core i7 7700 Intel CPU with a clock speed of 3.7 GHz, each analysis of the least complex (NBUCL&NSLIP model) and the most complex (BUCL&SLIPF model) model take approximately 3 and 15 minutes, respectively. The pushover curves of all 200 realizations of uncertain variables for the six considered models and for longitudinal and transverse wind directions are provided in Figs. 12 and 13. In addition, these figures show the mean and median load factor at each displacement increment in the pushover analysis. The mean and median curves, which represent the average behavior of tower, show that as expected buckling has a significant impact on the performance of the tower. In particular,

buckling decreases the load bearing capacity of the tower. In addition, joint slippage can significantly increase the lateral displacement while it slightly decreases the load bearing capacity of the tower. Among 200 realizations of uncertain variables there were a handful of extreme cases, in which connection failure occurs. However, these cases are rare and therefore, they do not affect the expected load bearing capacity of the tower. These extreme cases are discussed later in the next sub-section.

One major objective of this paper is to investigate the effect of modeling complexities on the performance of transmission towers. For this purpose, effects of buckling, joint slippage, and joint failure on load bearing capacity and lateral displacement of the tower is investigated. As mentioned previously, when wind is applied in longitudinal direction, the wind induced force on conductors is zero. However, since the tower is weaker about longitudinal axis (Fig. 11), the load bearing capacity of the tower about longitudinal axis is significantly lower than transverse axis. The actual values of load bearing capacity for each realization is obtained from Figs. 12 and 13 and the mean and standard deviation of load bearing capacity and the displacement corresponding to the load bearing capacity of the tower are presented in Table 8. A lognormal distribution is found to provide a good fit to the empirical distribution obtained from 200 pushover analyses. The probability density functions for load bearing capacity and displacement at load bearing capacity are also provided in Figs. 14 and 15. It should be noted that lateral displacement is an important criteria that has been used as a serviceability limit state for design and analysis of towers (Tessari et al., 2017; Kroetz et al., 2017). For both longitudinal and transverse wind, considering model NBUCL&NSLIP, the load bearing capacity of the tower is noticeably overestimated (Table 8). In this model, displacement-based beam-columns are used assuming large deformations, but the elements are not divided into four subelements and the initial imperfection is not applied. For longitudinal wind, comparing

model NBUCL&NSLIP with model BUCL, the mean load bearing capacity of the tower is reduced from 1.54 to 1.08, which shows a 30% reduction in the estimation of load bearing capacity of the tower. Similarly, for the transverse wind, the estimated mean load bearing capacity of the tower reduces from 2.57 to 1.9, which shows a 26% decrease. This confirms that in performance assessment of transmission towers, it is essential to divide each element into multiple sub-elements and apply initial imperfection to capture the buckling behavior of tower elements accurately. Moreover, for a longitudinal wind, considering slippage through model SLIP results in considerable increase in the lateral displacement of the tower. For example, for the longitudinal wind equal to design wind load of the tower (load factor equal to 1), the displacement of the tower from the mean curve in Fig. 12 is equal to 0.3 m and 0.35 m for model NBUCL&NSLIP and model SLIP, respectively, which shows a 16.7% increase in the lateral displacement of the tower. The same trend is observed for the transverse wind direction. It should be noted that model SLIP predicts the load bearing capacity of the tower as 1.41 times the design wind load of the tower, which shows a 8.5% reduction in the estimation of load bearing capacity compared to model NBUCL&NSLIP. This reduction is mostly attributed to additional P- Δ effects that occur due to excessive lateral displacement of the tower. However, model SLIP is still overestimating the load bearing capacity of the tower as it does not capture buckling effects accurately. For the longitudinal wind, model SLIPF shows a similar behavior to model SLIP as connection failure does not occur. However, for the transverse wind direction, the load bearing capacity reduces from 2.24 (in model SLIP) to 2.16 (in model SLIPF), which indicates a 4% reduction. This reduction is attributed to failure of connections. For the logitudinal wind as the tower is weaker about the longitudinal axis, steel elements fail before any connection failure occurs. On the other hand, for the transverse wind direction, as the tower is stronger about its transverse axis, in some cases,

connection failure occurs before tower elements fail and therefore, a failure mode due to rupture in connections occurs. Similar to longitudinal wind, model SLIP and SLIPF overestimate the load bearing capacity of the tower as they do not capture buckling effects accurately. In this case, for model NBUCL&NSLIP, SLIP, and SLIPF, in which buckling effect is not considered, the mean load bearing capacity is noticeably overestimated. For models BUCL&SLIP and BUCL&SLIPF, in which joint slippage and buckling effects are both accounted for, the load bearing capacity for longitudinal wind is 1.01, which shows a 6% reduction compared to model BUCL in which the load bearing capacity is equal to 1.08. This shows that joint slippage slightly reduces the expected load bearing capacity of the tower while joint failure does not affect the expected behavior. Additionaly, the lateral displacement of the tower is increased compared to model BUCL, as both buckling effects and joint slippage contribute to the lateral dispacement of the tower. For example, for a longitudinal wind, the lateral displacement of the tower for the load factor of 0.8 is 0.23, 0.27, 0.26, and 0.31 m for models NBUCL&NSLIP, BUCL, SLIP, and BUCL&SLIPF, respectively. The same trend is observed for the transverse wind direction. It should be noted that unlike models SLIP and SLIPF, in which the load bearing capacity of the tower is reduced for the transverse wind direction, if the connection failure is considered; for model BUCL&SLIP and BUCL&SLIPF, the estimated mean load bearing capacities are identical. This is due to the effect of buckling, as in most cases buckling occurs before the connection failure occurs, and therefore, connection failure is not controlling the expected load bearing capacity of the tower. As noted earlier, although the expected behavior of the tower (which is shown by mean pushover curves in Figs. 12 and 13) is not impacted by connection failure, for a handful of extreme cases, the connection failure occurs before a buckling failure mode is developed in the tower. To further investigate this effect, a post processing code in MATLAB is developed to present the state of tower elements and connections at multiple stages of pushover analyses obtained from OpenSEES. An approach to further validate the numerical models presented in this study is to compare results with experiments; however, due to lack of experimental data for the particular tower considered here, such comparisons are not made here. It should be noted that the failure modes and the performance of the tower has a good agreement with the observed performance of transmission towers in previous wind hazard events.

5.3 Effect of joint failure on failure of tower

In Fig. 16, the performance of the tower, assuming model *BUCL&SLIPF*, under a transverese wind force, for a single realization of uncertain variables that results in a connection failure mode is presented. As it was mentioned, this case is a rare case, in which connection failure was observed. For most of the analyses, connection failure does not occur (Figs. 12 and 13) and therefore, the average performance of the tower is not influenced by connection failure. This example, is provided to highlight the effect of connection failure on the extreme performance of the tower.

In Fig. 16, the state of tower elements is provided at three different points in the pushover responses. In this figure, damage is categorized into five different states. The elements shown with the magenta color are those that are under compression with a percentage of fibers yielded. These elements although partially yielded, (since some other fibers in the same section are still in their linear state) can undergo further compressive forces. Therefore, at this stage, although the element is damaged, it has not buckled yet. On the other hand, the red elements indicate that all the fibers in the cross section have yielded under the compressive force and the element cannot resist against any further loading. This state indicates the true buckling of the element. The elements with orange

color are the ones that are under tension but have partially yielded, while the elements in green are those with all their fibers have yielded under tensile forces. Therefore, this state is called plastic yielding. Additionally, joints that surpass their ultimate capacity are considered as failed and are shown with red circles. In Fig. 16, at point 1 (indicated by P1), the tower undergoes nonlinear behavior due to partial yielding (damage) in bracing and cage elements. However, since there is no failure mechnism developed in the tower, it can resist against further loading. At point 2, the tower experiences joint failure at the lap splices and buckling in the vicinity of the lap splice (joint). At this stage, the tower cannot resist against any further loading. At point 3, the elements are buckled and the tower is failed. In this case, the bearing capacity of the tower is equal to 2.09 times the design load of the tower. Although this mode of failure is not common, for decayed towers with rusted bolts and joint elements, joint failure can occur as rusted connections have lower capacity compared to their design capacity. Joint failure was also observed in a set of experimental analyses of steel towers performed by Szafran (2015). Moreover, in model BUCL, in which both joint slippage and joint failure are neglected (Fig. 17), at point 1, there are a couple of bracing elements that exhibit nonlinear behaviors (partial damages), however, as the true buckling has not occurred at that point, the tower has not yet failed. At point 2, several leg, cage and bracing elements experience nonlinear behaviors but the tower has not failed as the main elements in the leg and in the cage have not failed. Finally, at point 3, the tower fails due to the buckling of the leg elements at the bottom of the tower. At this stage, a failure mechanism is developed in the main elements of the tower and therefore the tower is collapsed. Using model BUCL the estimated load bearing capacity is equal to 2.1 times the design load of the tower. Therefore, the joint slippage is not noticeably changing the load bearing capacity of the tower. However, it changes the failure mode. A change in the failure mode is an important consideration especially for life cycle assessment procedures that involve estimation of repair time, which affect the duration of outage and therefore, the associtated repair costs. Moreover, capturing the true failure mechanism is important for reliability and resilience improvement strategies, as a change in the failure mode can completely change the enhancement strategy. It should be noted that in Figs. 16 and 17 to present the state of the tower more clearly, the displacements of the tower are overexaggereated, but the true displacements are considered for analysis.

5.4 Effect of uncertainty on failure of the tower

The impact of uncertainty on the performance of towers are investigated through Table 8 and Figs. 12-15. However, these figures do not specifically present the state of tower elements and the impact of uncertainty on the number of failures in the tower. The state of tower elements at the failure instance in all 200 pushover analyses is presented through Fig. 19. In this figure, the thickness of each failed element and the diameter of the circle shows the number of failures (including buckling, plastic yielding, and connection failure) occurred in the corresponding element. For example, if a buckled element is thicker than another buckled element, it shows that a larger number of buckling failures have occurred in that element. In addition, the elements shown by blue lines are the elements that failure has not occurred in them in all 200 analyses. Considering a longitudinal wind, two significant failure modes are observed. First, failure due to buckling in the cage elements, and failure due to buckling in leg elements (Fig 19.a). As noted previously, these modes of failure have been observed in previous failure events (Elks, 2016; IEEE TP&C line design, 2018) as well as experimental analyses of towers (Rao et al., 2012). For the transmission tower studied in this analysis, the leg elements are made of high strength A242 steel with a yield strength of 50 ksi while the cage

elements are made of conventional A36 steel with a yield strength of 36 ksi. Therefore, more failures are expected to occur in the cage. In addition, as it was mentioned previously, a handful of connection failures occur in a lap-splice that is shown with black circle. Moreover, for a transverse wind, most of the failures occur in the cage elements while there are a handful of failures in the leg elements, mid height elements and connections (fig. 19.b). More connection failure is observed for transverse wind direction. This is due to the weakness of the tower about its longitudinal axis, which causes the tower elements to buckle before connection failure occurs in the tower. It should be noted that Fig. 19 highlights the importance of tower elements in the failure of the tower, and subsequently can provide a better understanding on how to enhance the robustness of the tower. For example, it was observed that the cage elements often buckle and control the failure of the tower. Therefore, to improve the performance of the tower, these elements could be replaced by high strength A242 steel elements. As mentioned earlier, the objective of this paper is to investigate the effect of modeling complexities and uncertainties on the wind performance of transmission towers. However, investigating strengthening strategies is beyond the scope of the present study. These effects will be investigated in future studies. The modelling approach proposed in this study could be integrate with advanced reliability analysis techniques (Darestani et al., 2019; Zamanian, 2016; Rahimi et al., 2019; Sichani and Padgett 2019; Sichani et al., 2018) to generate fragility models for transmission towers.

6. Summary and Conclusions

This study investigated the impact of uncertainties in demand and capacity along with various modeling complexities such as buckling, joint slippage and joint failure on the extreme wind performance of transmission towers. For this purpose, 200 realizations

of uncertain variables are generated through LHS method and the performance of the tower is investigated through six different models using nonlinear Finite Element static pushover analyses in OpenSEES. Each of these six models considers a set of modeling complexities. In order to consider buckling, each element is divided into four subelements and an initial imperfection is applied to the additional nodes. Furthermore, a nonlinear joint slippage connection model is proposed using Zerolength elements in OpenSEES. This model is capable of capturing failure in the connections by defining a drop in the backbone curve of the joint slippage model. The simplest model neglects buckling and joint slippage effects, while these along with failure of joints are considered in the most accurate of the six developed models.

Results of this study indicated that buckling can noticeably impact the response of transmission towers. Particularly, buckling, on average, decreases the load bearing capacity of the tower by up to 30%. Joint failure does not noticeably decrease the load bearing capacity of lattice towers. However, in rare cases, it can change the mode of failure and therefore, it can impact the strengthening strategy. In addition, joint slippage slightly affects the load bearing capacity of towers by up to 6%, while it significantly increases the lateral displacement of the tower, which can affect the serviceability of transmission towers. Consequently, for risk and resilience assessment of steel lattice transmission towers, especially for capturing small probabilities of failure, it is imperative to have a model that is capable of capturing buckling effects, joint slippage, and joint failure.

It should be noted that connections are very often designed to be stronger than their connected elements to make sure that connection failure does not occur before the elements fail. However, in reality, due to uncertainties in the behavior of connections and construction errors, among other factors, it is possible that connections fail before the

attached elements fail. Therefore, in probabilistic analysis of transmission towers, connection failure should be considered as it may impact the extent of damage and the mode of failure. Furthermore, results of this study confirmed that the collapse of the tower is commonly associated with the buckling of the main elements of the tower including the leg elements or vertical elements of the cage. Prior to this failure, several elements may experience partial damage. The knowledge of these component-level damages can be leveraged to devise effective strengthening and recovery procedures. It should be noted that the derived conclusions are specifically applicable to the assumed tower configuration and material properties. Further investigations are needed to fully characterize impacts of uncertainties and modeling complexities on the extreme wind hazard performance of lattice transmission towers with different configurations and material properties.

Acknowledgement

This paper is based upon work supported by the National Science Foundation under Grants No. CMMI-1635569 and CMMI-1762918. This support is greatly appreciated.

References

- ASCE 07, Minimum design loads for buildings and other structures. American Society Civil Engineers (ASCE). Reston, VA, USA; (2016)
- ASCE No. 74 (2009) "Guidelines for Electrical Transmission Line Structural Loading" American Society of Civil Engineers.
- Bhat R., Y. Mohammadi Darestani, A. Shafieezadeh, A.P. Meliopoulos, R. DesRoches. "Resilience Assessment of Distribution Systems Considering the Effect of Hurricanes", IEEE PES Transmission and Distribution Conference & Exposition. Denver, Co. USA. April 16-19, 2018
- Campbell R. J., "Weather-related power outages and electric system resiliency," Congressional Research Service, Library of Congress, R42696, Aug. 2012.
- Darestani, Y. M., and A. Shafieezadeh. "Multi-dimensional wind fragility functions for wood utility poles." Engineering Structures 183 (2019a): 937-948.
- Darestani, Y. M., and A. Shafieezadeh. "Modeling the Impact of Adjacent Spans in Overhead Distribution Lines on the Wind Response of Utility Poles." In Geotechnical and Structural Engineering Congress 2016a, pp. 1067-1077.
- Darestani, Y.M, A. Shafieezadeh, and R. DesRoches. "An equivalent boundary model for effects of adjacent spans on wind reliability of wood utility poles in overhead distribution lines." Engineering Structures 128 2016b: 441-452.
- Darestani, Y. M., A. Shafieezadeh, and R. DesRoches. "Effects of Adjacent Spans and Correlated Failure Events on System-Level Hurricane Reliability of Power Distribution Lines." IEEE Transactions on Power Delivery 2017.
- Darestani, Y. M., and A. Shafieezadeh, "Hurricane Performance Assessment of Power Distribution Lines Using Multi-scale Matrix-based System Reliability Analysis Method", 13th Americas Conference on Wind Engineering, Gainesville, Florida, USA, May 21 24, 2017
- Darestani, Y. M., and A. Shafieezadeh. "A Framework for Hurricane Resilience Assessment of Power Distribution Systems." (2019b).
- Darestani, Y. M., Z. Wang, and A. Shafieezadeh. "Wind Reliability of Transmission Line Models using Kriging-Based Methods." (2019).
- De Souza RR, Fleck LFM, Kaminski J, Lopez RH. Topology design recommendations of transmission line towers to minimize the bolt slippage effect. ENGINEERING STRUCTURES 178, 286-297, 2019.
- Sichani, M. E., and J. E. Padgett. "Surrogate modelling to enable structural assessment of collision between vertical concrete dry casks." Structure and Infrastructure Engineering (2019): 1-14.
- Sichani, M. E., J. E. Padgett, and V. Bisadi. "Probabilistic seismic analysis of concrete dry cask structures." Structural Safety 73 (2018): 87-98.
- Elks, S., "Floods live: Thames and Severn rising fast," The Times, 07-Jan-2016. [Online]. Available:
 - http://www.thetimes.co.uk/tto/multimedia/archive/00522/147453653__522161b.jp g. [Accessed: 07-Jan-2016].
- Ellingwood B. R., and P. B. Tekie. "Wind load statistics for probability-based structural design." journal of Structural Engineering 125, no. 4: 453-463, (1999).
- Fang, S., S. Roy, and Jacob Kramer. "Transmission structures." Structural engineering handbook (1999).
- Fu, X. and Li, H.N., 2018. Uncertainty analysis of the strength capacity and failure path for a transmission tower under a wind load. Journal of Wind Engineering and Industrial Aerodynamics, 173, pp.147-155.

- Hoffman P. and W. Bryan, "Comparing the impacts of Northeast hurricanes on energy infrastructure," Office of Electricity Delivery and Energy Reliability, U.S. Department of Energy, Apr. 2013.
- IEEE TP&C Line Design," Nov-20-2018. [Online]. Available: http://www.oocities.org/ieee tpc/ieee photos/photos.htm. [Accessed: 11-20-2018].
- Jiang, W. Q., Z. Q. Wang, G. McClure, G. L. Wang, and J. D. Geng. "Accurate modeling of joint effects in lattice transmission towers." Engineering Structures 33, no. 5 (2011): 1817-1827.
- Jiang, Wen-Qiang, Yao-Peng Liu, Siu-Lai Chan, and Zhang-Qi Wang. "Direct Analysis of an Ultrahigh-Voltage Lattice Transmission Tower Considering Joint Effects." Journal of Structural Engineering 143, no. 5 (2017): 04017009.
- Kaminski Jr, J., J. D. Riera, R. C. R. de Menezes, and Letícia FF Miguel. "Model uncertainty in the assessment of transmission line towers subjected to cable rupture." Engineering Structures 30, no. 10 (2008): 2935-2944.
- Kempner Jr, L., W. H. Mueller III, S. Kitipornchai, F. Albermani, R. C. De Menezes, and J. B. G. F. Da Silva. "Lattice transmission tower analysis: beyond simple truss model." American Society of Civil Engineers, 2002.
- Kitipornchai, S., Al-Bermani, F. G. A., & Peyrot, A. H. (1994). Effect of bolt slippage on ultimate behavior of lattice structures. Journal of structural engineering, 120(8), 2281-2287.
- Kroetz, H. M., R. K. Tessari, and A. T. Beck. "Performance of global metamodeling techniques in solution of structural reliability problems." Advances in Engineering Software 114 (2017): 394-404.
- McKenna F, Fenves GL, Scott MH. Open system for earthquake engineering simulation (OpenSEES). Berkeley, CA: University of California; 2000.
- McKenna, F. "OpenSees: a framework for earthquake engineering simulation." Computing in Science & Engineering 13, no. 4 (2011): 58-66.
- Rao, N.P., Knight, G.S., Mohan, S.J. and Lakshmanan, N., 2012. Studies on failure of transmission line towers in testing. Engineering structures, 35, pp.55-70.
- Rahimi, M., Z. Wang, A. Shafieezadeh, D. Wood, and E. J. Kubatko. "An Adaptive Kriging-Based Approach with Weakly Stationary Random Fields for Soil Slope Reliability Analysis." In Geo-Congress 2019: Soil Erosion, Underground Engineering, and Risk Assessment, pp. 148-157. Reston, VA: American Society of Civil Engineers, 2019.
- Rezaei, S.N., Chouinard, L., Langlois, S. and Légeron, F., 2016. Analysis of the effect of climate change on the reliability of overhead transmission lines. Sustainable Cities and Society, 27, pp.137-144.
- Rezaei, S. N., L. Chouinard, S. Langlois, and F. Légeron. "A probabilistic framework based on statistical learning theory for structural reliability analysis of transmission line systems." Structure and Infrastructure Engineering 13, no. 12 (2017): 1538-1552.
- Szafran, J., 2015. An experimental investigation into failure mechanism of a full-scale 40 m high steel telecommunication tower. Engineering Failure Analysis, 54, pp.131-145.
- Tapia-Hernández, E., S. Ibarra-González, and D. De-León-Escobedo. "Collapse mechanisms of power towers under wind loading." Structure and Infrastructure Engineering 13, no. 6 (2017): 766-782.
- Tapia-Hernández E., and E. Sordo. "Structural behaviour of lattice transmission towers subjected to wind load." Structure and Infrastructure Engineering 13, no. 11 (2017): 1462-1475.

- Tessari, R. K., H. M. Kroetz, and A.T. Beck. "Performance-based design of steel towers subject to wind action." Engineering Structures 143 (2017): 549-557.
- Ungkurapinan, N. (2000). A Study of Joint Slip in Galvanized Bolted Angle Connections, MSc. Thesis, University of Manitoba, Winnipeg, Canada.
- Uriz, P., Filippou, F. C., & Mahin, S. A. (2008). Model for cyclic inelastic buckling of steel braces. Journal of structural engineering, 134(4), 619-628.
- Wang, F. Y., Y. L. Xu, and S. Zhan. "Concurrent multi-scale modeling of a transmission tower structure and its experimental verification." Advanced Steel Construction 13 (2017): 258-272.
- Zamanian, S. "Probabilistic Performance Assessment of Deteriorating Buried Concrete Sewer Pipes." PhD diss., The Ohio State University, 2016.

Table 1. Convergence study on the number of discretizations for accurate estimation of the buckling force in OpenSEES for the case of simply support 1.75X1.25X0.1875 angle section element

Simply supported		Imperfec	ction Camber Displac	ement (*Le	ength)		Theoretica
element	0.00001		0.0005		0.001		Buckling
lf .l	Buckling Force	Error	Buckling Force	Error	Buckling	Error	Force (kN)
number of elements	(kN)	(%)	(kN)	(%)	Force (kN)	(%)	roice (KIN)
2	3.94	20.1	3.90	18.9	3.87	18.0	-
4	3.42	4.3	3.39	3.4	3.36	2.4	3.28
8	3.29	0.3	3.26	-0.6	3.23	-1.5	3.28
16	3.26	-0.6	3.23	-1.5	3.20	-2.4	

Table 2. Convergence study on the number of discretizations for accurate estimation of the buckling force in OpenSEES for the case of fixed end 1.75X1.25X0.1875 angle section element

fix supported		Imperfec	ction Camber Displac	ement (*Le	ength)		Theoretica
element	0.00001		0.0005		0.001		Buckling
1 61 4	Buckling Force	Error	Buckling Force	Error	Buckling	Error	Force (kN)
number of elements	(kN)	(%)	(kN)	(%)	Force (kN)	(%)	Force (KIN)
2	15.79	20.4	15.45	17.8	15.15	15.5	
4	15.80	20.4	15.45	17.8	15.15	15.5	12.12
8	13.69	4.3	13.45	2.5	13.25	1.0	13.12
16	13.16	0.3	12.96	-1.2	12.77	-2.7	

Table 3. Convergence study on the number of discretizations for accurate estimation of the buckling force in OpenSEES for the case of simply support 4X4X0.3125 angle section element

Simply supported		Imperfec	ction Camber Displac	ement (*Le	ength)		Theoretica
element	0.00001		0.0005		0.001		Buckling
number of elements	Buckling Force	Error	Buckling Force	Error	Buckling	Error	Force (kN
number of elements	(kN)	(%)	(kN)	(%)	Force (kN)	(%)	roice (kiv
2	570.44	39.1	483.06	17.8	447.59	9.2	
4	510.70	24.6	443.72	8.2	410.78	0.2	410
8	491.37	19.8	431.73	5.3	399.52	-2.6	410
16	486.78	18.7	428.65	4.5	396.75	-3.2	

Table 4. Convergence study on the number of discretizations for accurate estimation of the buckling force in OpenSEES for the case of fixed end 4X4X0.3125 angle section element

Simply supported		Imperfec	ction Camber Displac	ement (*Le	ength)		Theoretica
element	0.00001		0.0005		0.001		Buckling
	Buckling Force	Error	Buckling Force	Error	Buckling	Error	Force (kN
number of elements	(kN)	(%)	(kN)	(%)	Force (kN)	(%)	roice (kiv
2	582.60	8.1	576.70	7.0	570.87	5.9	
4	582.63	8.1	576.14	6.9	569.79	5.7	539
8	582.56	8.1	572.93	6.3	563.65	4.6	339
16	582.54	8.1	572.00	6.1	561.87	4.2	

Table 5. Uncertain variables defining material behavior and wind loading

	Properties	Notation	Type of Distribution	Mean	COV	Reference
	Modulus of elasticity	E	LogNormal	2.0e11 (N/m ²)	0.06	
Steel	Yield stress of main leg	f_{ym}	LogNormal	4.02e8(N/m ²)	0.1	-
material	Yield stress of other elements	f_{yb}	LogNormal	2.9e8 (N/m²)	0.1	ASCE07 (2016) and - ASCE 74 (2009)
	Post yield elasticity	$\boldsymbol{E_{st}}$	LogNormal	0.02E(N/m ²)	0.25	ASCL /4 (2007)
Buckling	Imperfection of element		Uniform	0.075(%)	0.192	
	Gust effect factor	G	Normal	Section 3	0.11	
Wind	Force coefficient	C_f	Normal	Section 3	0.12	ASCE07 (2016),
load	Velocity pressure exposure coefficient	Kz	Normal	Section 3	0.16	Ellingwood and Tekie (1999) and
	Wind directionality factor	K_d	Normal	Section 3	0.08	=

Table 6. Uncertain variables defining connections

	D (*	NI 4 "	Type of			D. f.
]	Properties	Notation	Distribution	Mean	COV	Reference
	Load at onset of slip	Force @ A*	LogNormal	86.6 kN	0.109	
	Load at end of slip	Force @ B*	LogNormal	197.3 kN	0.23	=
	Load at onset of plasticity	Force @ C*	LogNormal	317 kN	0.13	=
a	Maximum load	Force @ D*	LogNormal	440 kN	0.017	-
Connection Type A	Dis. at elastic frictional load transfer	Phase 1	LogNormal	0.29 mm	0.35	_
	Slippage length	Phase 2	Uniform	1.9 mm	0.61	<u>-</u>
	Dis. at elastic load transfer	Phase 3	LogNormal	2.95(mm)	0.27	-
	Dis. at nonlinear load transfer	Phase 4	LogNormal	0.36(mm)	0.34	
	Load at onset of slip	Force @ A	LogNormal	23.95(kN)	0.1	-
	Load at onset of plasticity	Force @ C	LogNormal	132.17(kN)	0.09	_
	Maximum load	Force @ D	LogNormal	205.08(kN)	0.02	=
Connection Type B	Dis. at elastic frictional load transfer	Phase 1	LogNormal	0.11(mm)	0.1	_
Турс В	Slippage length	Phase 2	Uniform	0.45(mm)	0.15	=
	Dis. at elastic load transfer	Phase 3	LogNormal	2.09(mm)	0.22	_
	Dis. at nonlinear load transfer	Phase 4	LogNormal	3.99(mm)	0.16	_
-	Load at onset of slip	Force @ A	LogNormal	9.29(kN)	0.084	_
	Load at onset of plasticity	Force @ C	LogNormal	65.03(kN)	0.098	
	Maximum load	Force @ D	LogNormal	107.78(kN)	0.039	Ungkurapinan (200
Connection	Dis. at elastic frictional load transfer	Phase 1	LogNormal	0.39(mm)	0.29	
Type C1	Slippage length	Phase 2	Uniform	1.28(mm)	0.43	
	Dis. at elastic load transfer	Phase 3	LogNormal	2.74(mm)	0.175	
	Dis. at nonlinear load transfer	Phase 4	LogNormal	6.04(mm)	0.158	_
	Load at onset of slip	Force @ A	LogNormal	20.14(kN)	0.219	_
	Load at onset of plasticity	Force @ C	LogNormal	97.51(kN)	0.115	=
	Maximum load Dis. at elastic	Force @ D	LogNormal	157.71(kN)	0.062	_
Connection	frictional load transfer	Phase 1	LogNormal	0.25(mm)	0.26	
Type C2	Slippage length	Phase 2	Uniform	1.32(mm)	0.44	-
	Dis. at elastic load transfer	Phase 3	LogNormal	1.73(mm)	0.225	-
	Dis. at nonlinear load transfer	Phase 4	LogNormal	2.55(mm)	0.235	_
	Load at onset of slip	Force @ A	LogNormal	29.28(kN)	0.069	=
-	Load at onset of plasticity	Force @ C	LogNormal	152.85(kN)	0.095	_
	Maximum load	Force @ D	LogNormal	204.4(kN)	0.117	_
Connection Type C3	Dis. at elastic frictional load transfer	Phase 1	LogNormal	0.28(mm)	0.28	_
1 ype C3	Slippage length	Phase 2	Uniform	1.11(mm)	0.37	=
	Dis. at elastic load transfer	Phase 3	LogNormal	2.4(mm)	0.192	=
	Dis. at nonlinear load transfer	Phase 4	LogNormal	2.18(mm)	0.174	

^{*}Adjusted to account for lap splices with 8 bolts

Table 7. Various models developed in OpenSEES

Model No.	Divid Compostion	Dualdina	Semi-rigid connection			
Model No.	Rigid Connection	Buckling	Without failure	With failure		
NBUCL&NSLIP*	✓					
BUCL*	✓	✓				
SLIP*			✓			
SLIPF*				✓		
BUCL&SLIP*		✓	✓			
BUCL&SLIPF*		✓		✓		

^{*}NBUCL: No Buckling, NSLIP; No Slippage, BUCL: Buckling, SLIP: Slippage, SLIPF: Slippage with failure in connection

Table 8. Comparison of bearing capacity and displacement of tower models from Figs. 12-13

Model	Wind Direction -	Load bearing capacity (Factor)		Displacement at bearing capacity (m)		
	Direction	Mean	STD	Mean	STD	
NBUCL&NSLIP*	Transverse	2.57	0.65	0.61	0.11	
BUCL*	Transverse	1.9	0.46	0.30	0.03	
SLIP*	Transverse	2.24	0.56	0.47	0.10	
SLIPF*	Transverse	2.16	0.53	0.40	0.05	
BUCL&SLIP*	Transverse	1.85	0.45	0.34	0.04	
BUCL&SLIPF*	Transverse	1.85	0.45	0.34	0.04	
NBUCL&NSLIP	Longitudinal	1.54	0.42	0.81	0.13	
BUCL	Longitudinal	1.08	0.30	0.41	0.07	
SLIP	Longitudinal	1.41	0.41	0.67	0.09	
SLIPF	Longitudinal	1.42	0.41	0.69	0.09	
BUCL&SLIP	Longitudinal	1.01	0.27	0.46	0.11	
BUCL&SLIPF	Longitudinal	1.01	0.27	0.46	0.10	

^{*}NBUCL: No Buckling, NSLIP; No Slippage, BUCL: Buckling, SLIP: Slippage, SLIPF: Slippage with failure in connection

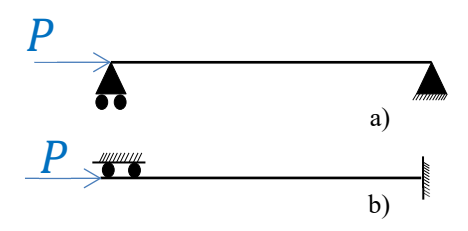


Figure 1. Beams for the verification of modeling buckling in OpenSEES a) pinned ends (simply supported) and b) fixed ends

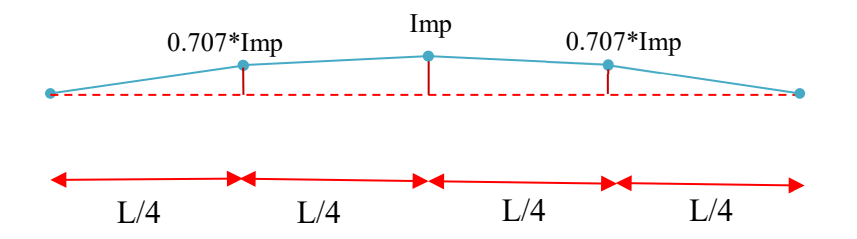


Figure 2. Discretization and imperfection modeling of lattice elements to capture buckling in OpenSEES

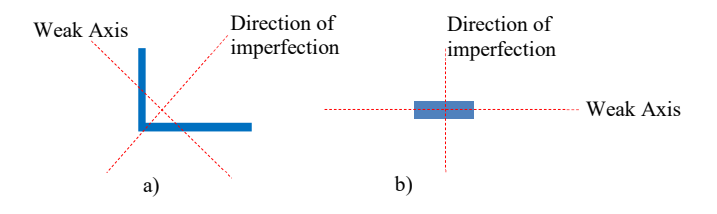


Figure.3 The direction of imperfection with respect to the cross section

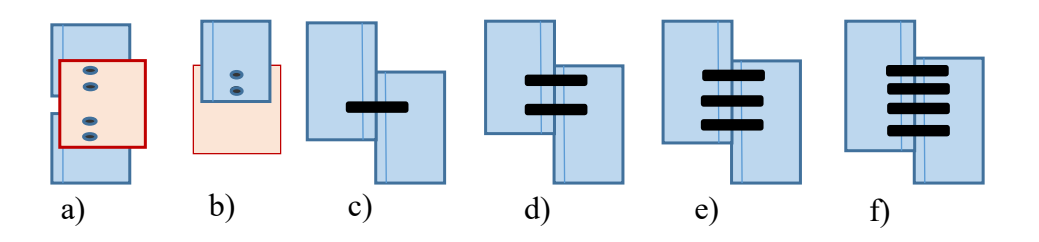


Figure 4. Connections reported by Ungkurapinan (2000) a) Type A b) Type B c) Type C1 d) Type C2 e) Type C3 f) Type C4

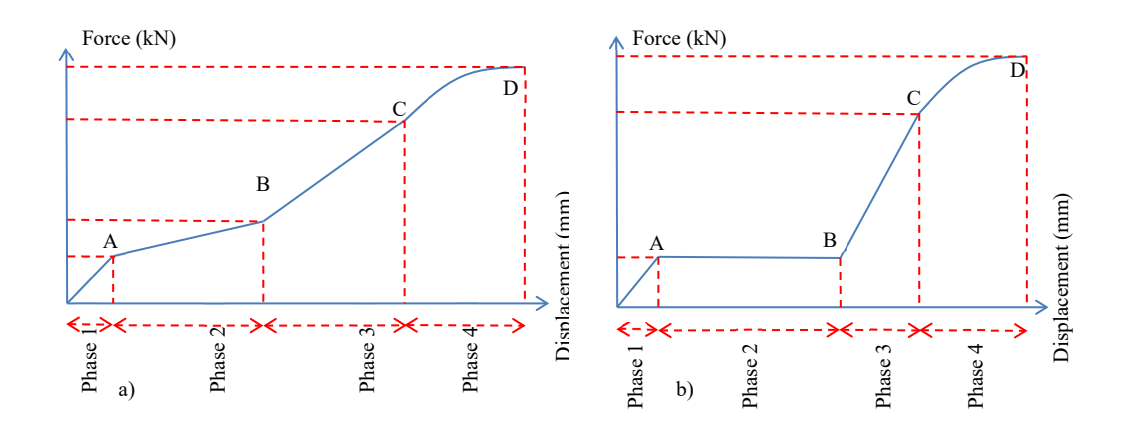


Figure 5. Backbone curve for connection a) Type A b) Type B and C (Ungkurapinan, 2000)

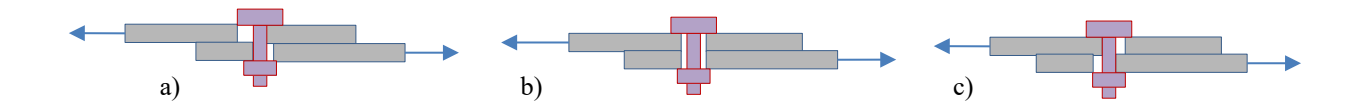


Figure 6. Different clearance levels a) minimum b) normal c) maximum

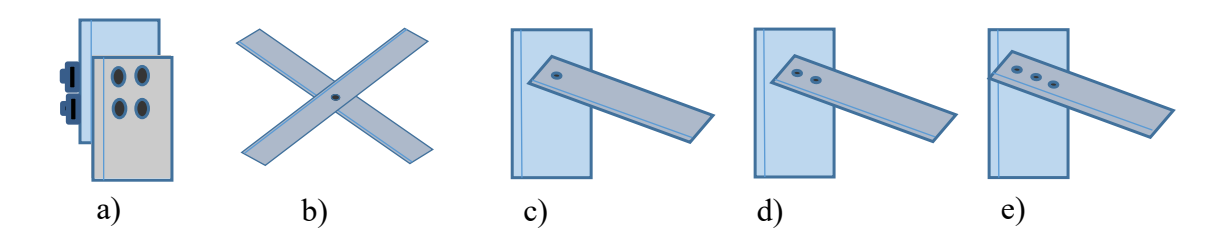


Figure 7. Connections considered in this study a) lap Splices b) bracing to bracing c) bracing to main element (1 bolt) d) bracing to main element (2 bolts) e) bracing to main element (3 bolts)

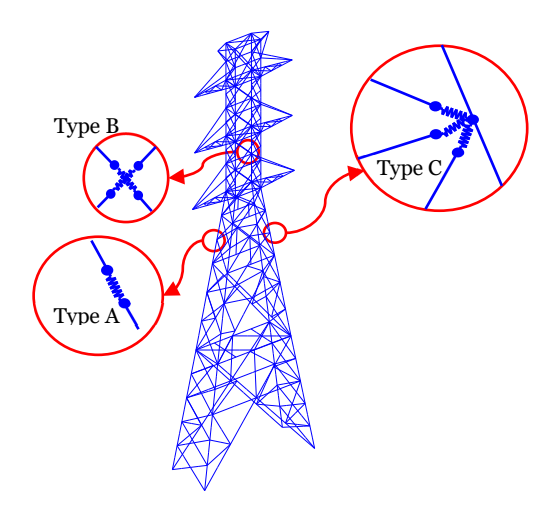


Figure 8. Modeling semi-rigid connections in OpenSEES using Zerolength elements.

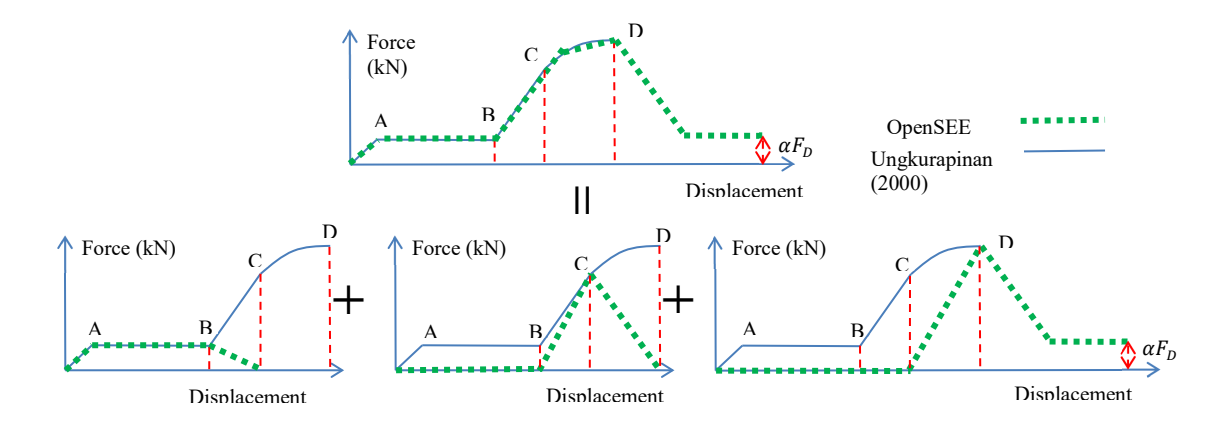


Figure 9. Developing connection material in OpenSEES

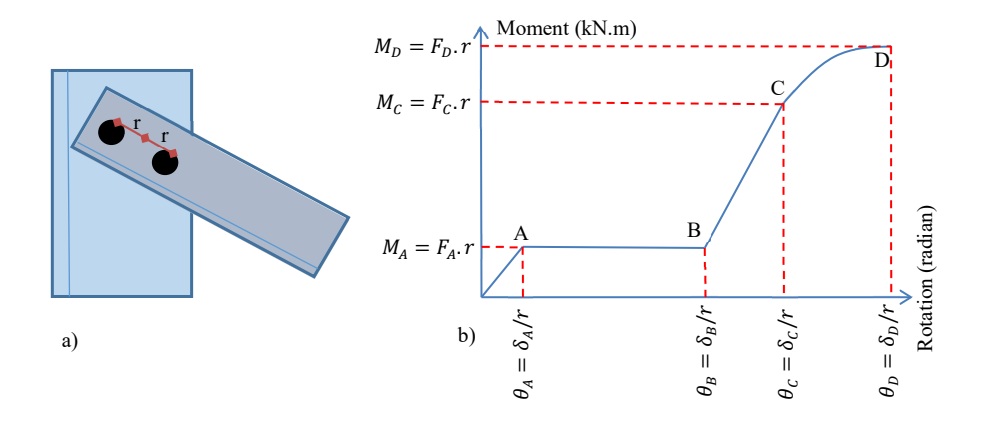


Figure 10. The configuration of a typical connection for the derivation of moment-rotation relationships a) calculation of r for a joint with two bolts b) moment-rotation behavior of a single bolt

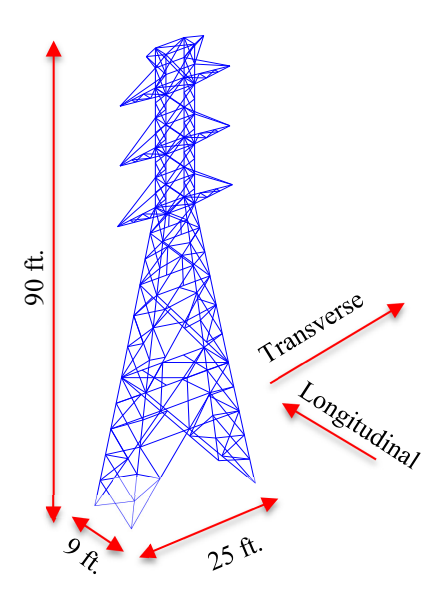


Figure 11. Double circuit lattice tower assumed in this study

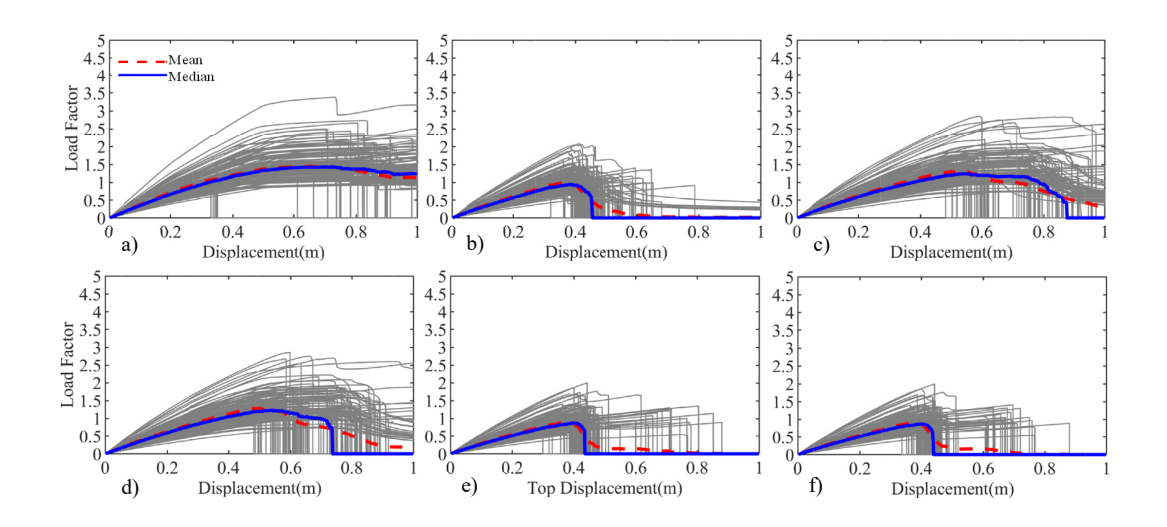


Figure 12. Pushover curves for longitudinal wind direction for models a) NBUCL&NSLIP b) BUCL c) SLIP d) SLIPF e) BUCL&SLIP f) BUCL&SLIPF

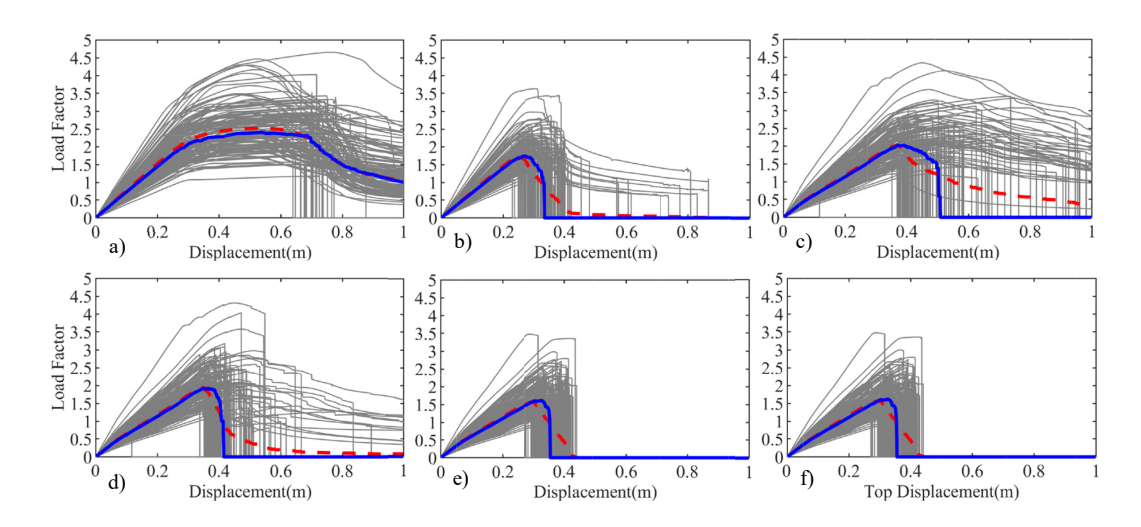


Figure 13. Pushover curves for transverse wind direction for models a) NBUCL&NSLIP b) BUCL c) SLIP d) SLIPF e) BUCL&SLIP f) BUCL&SLIPF

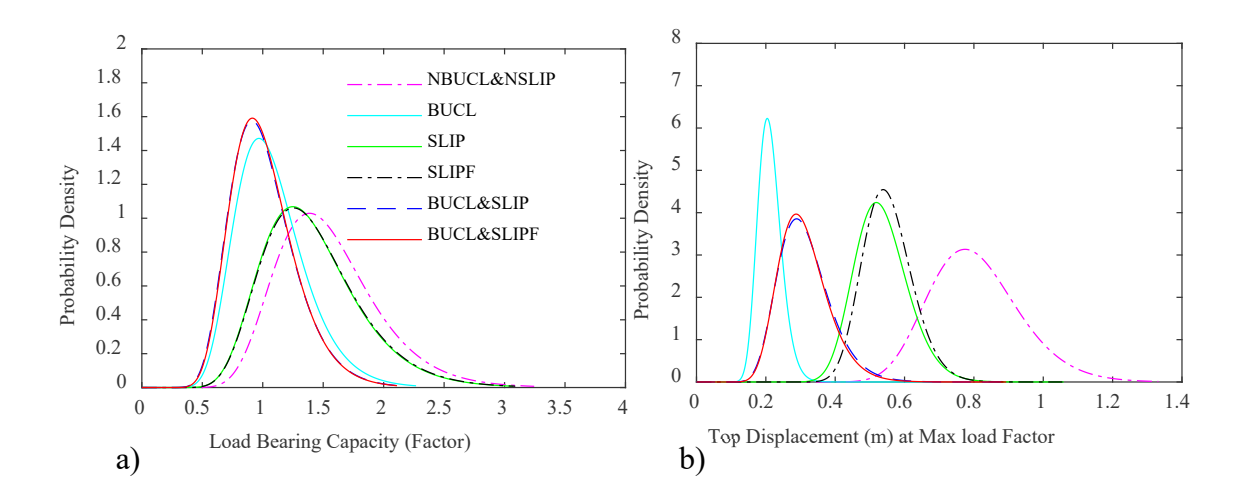


Figure. 14 Probability density function of load bearing capacity and displacement at max load capacity (longitudinal wind)

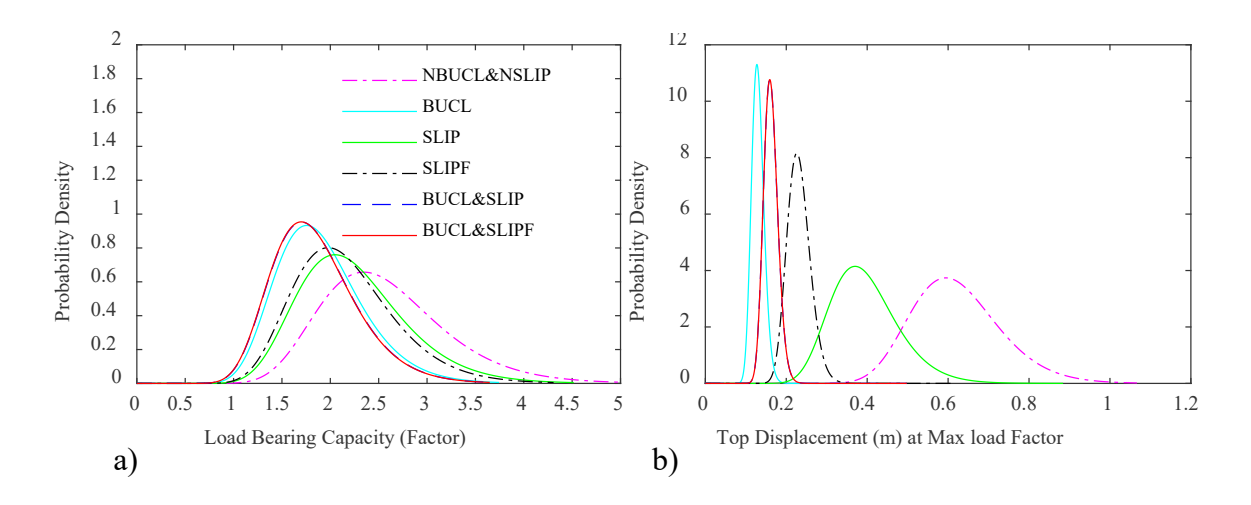


Figure. 15 Probability density function of load bearing capacity and displacement at max load capacity (transverse wind)

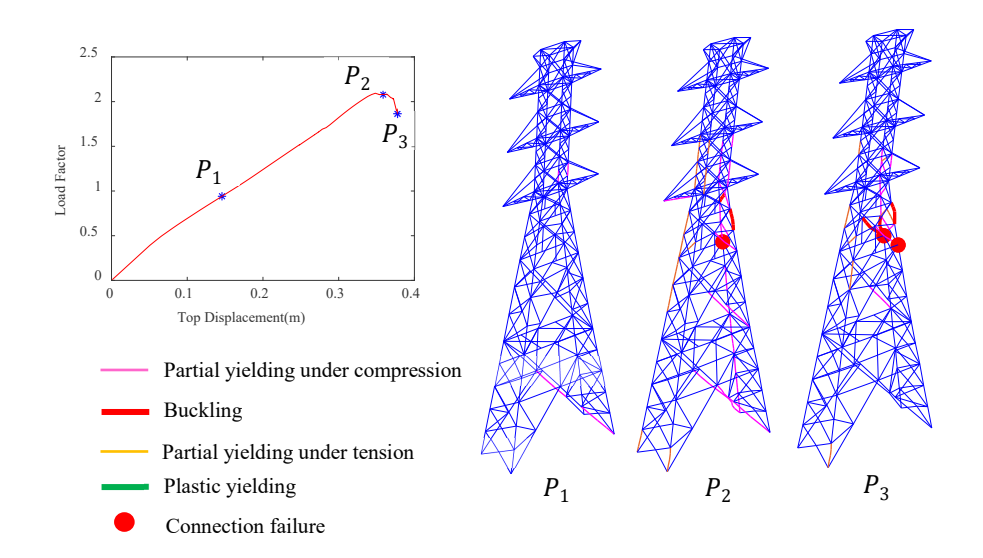


Figure 16. Investigation of failure mechanism for transverse wind direction assuming model BUCL&SLIPF

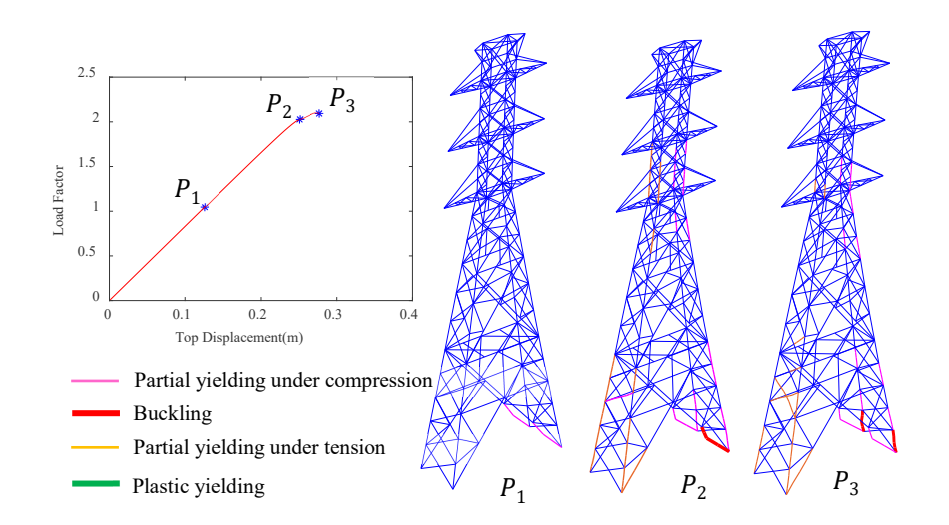


Figure 17. Investigation of failure mechanism for transverse wind direction assuming model BUCL

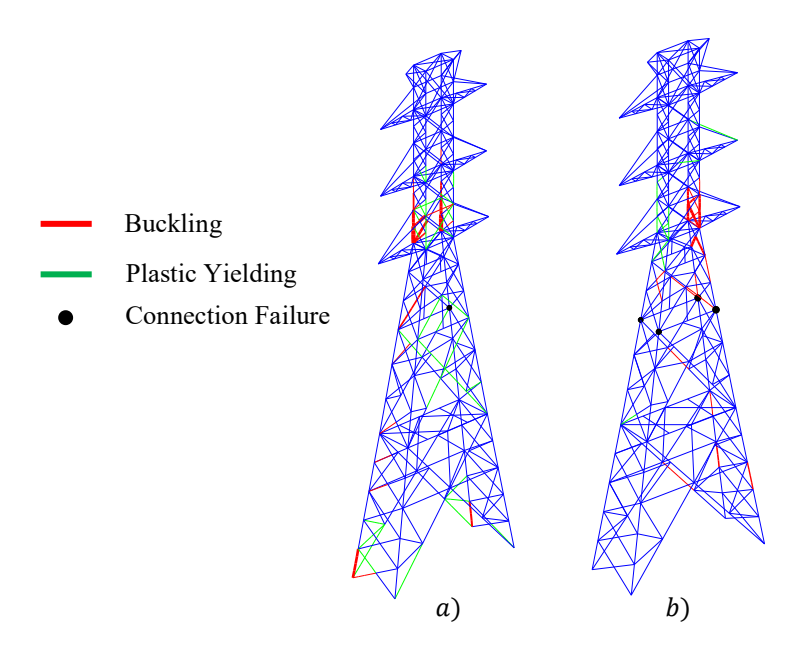


Figure 18. The type and location of damaged components in the transmission tower derived from 200 pushover analyses for a) longitudinal wind and b) transverse wind